Melting of Wüstite and Iron up to Pressures of 600 kbar

Guoyin Shen, Peter Lazor, and Surendra K. Saxena

Theoretical Geochemistry Program, Department of Mineralogy and Petrology, Institute of Earth Sciences, P.O. Box 555, Uppsala University, S-752 36 Uppsala, Sweden

Abstract. The effect of pressure on melting temperature of wüstite and iron has been measured with laser-heated diamond anvil cell. The temperature was determined by measuring the thermal radiation emitted by the sample as a function of wavelength in the range from 600 nm to 900 nm to which Planck's radiation function was fitted; the pressure was measured by ruby-fluorescence technique. The melting curve of wüstite in this study when extrapolated to low pressures agrees with Lindsley's (1966) data. Our data are similar to the recent data of Boehler (1992) and close to that of Ringwood and Hibberson (1990) at pressure of 160 kbar, but the melting temperature does not rise as rapidly with increasing pressure as reported by Knittle and Jeanloz (1991). If tungsten emissivity is used in the temperature calculation, the melting curve of iron matches those of Boehler et al. (1990). Use of emissivity of iron in the temperature calculation results in somewhat higher temperatures than those reported by Boehler et al. (1990).

Introduction

Melting is one of the important processes in the evolution of planets. With the technique of laser-heated diamond anvil cell, the melting curves of a few geophysically important materials, e.g., iron, wüstige and perovskite, have been obtained to extremely high pressures which are close to that of the core-mantle boundary (e.g., Heinz and Jeanloz 1987; Williams et al. 1987; Boehler et al. 1990). Such static experiments give us a chance to place constraints on the physical and chemical properties of the materials at the core-mantle boundary or even in the deep core in the earth.

Melting of wüstite has been experimentally studied by Lindsley (1966) at pressures up to 30 kbar with piston-cylinder apparatus, by Ringwood and Hibberson (1990) at a pressure of 160 kbar with multi-anvil press, by Knittle and Jeanloz (1991) up to 1000 kbar with laser-

heated diamond anvil cell (DAC) and recently by Boehler (1992) up to 500 kbar with laser heated DAC. The melting temperature at 160 kbar by Knittle and Jeanloz (1991) is about 700 K higher than that reported by Ringwood and Hibberson (1990) and Boehler (1992). Boehler (1992) found that melting temperature at 500 kbar is 1100 K lower than that measured by Knittle and Jeanloz (1991). The melting curves of iron as determined by different authors could also be quite different. The melting temperature at 1 Mbar as measured by Boehler et al. (1990) differ from those of Williams et al. (1991), both with the laser-heated DAC technique, by over 1000 K. Such a large discrepancy may be due to the use of different methods of detecting melting and determination of temperature and pressure. In order to resolve these differences, we have measured the melting temperatures of wüstite and iron up to a pressure of 600 kbar with laser-heated diamond anvil cell.

Experimental Procedures

Samples Preparation

Wüstite. Wüstite with the composition $Fe_{0.94}O$ used in our experiments was provided by E. Hålenius. The sample was synthesized from hematite with controled oxygen fogacity at 1000° C. The sample was later ground into a powder. $Fe_{0.94}O$ was characterized by X-ray diffraction with cell parameter a as 4.307 Å.

Stainless steel T301 gasket was used for laser-heating experiments. Prior to an experiment, the gasket was indented between diamond anvils with pressures about 100 kbar at the centre, and a 250 μm diameter hole was drilled at the centre of the indention. The thickness after indention was about 100 μm. The wüstite powder was loaded into the gasket hole. A ruby chip (about 100 μm × 100 μm) was then put over the sample (Fig. 1a). This ruby chip is used for measuring the pressure directly on the spot and isolating the sample from the diamonds. At low pressures, the reaction between FeO and Al_2O_3 to form hercynite, $FeAl_2O_4$, is possible. However, most of the present experiments were carried out at pressures above 150 kbar where hercynite is unstable. Heinz and Jeanloz (1987) observed that the ruby-fluorescence signal degrades continually as each time the sample is heated. But we found
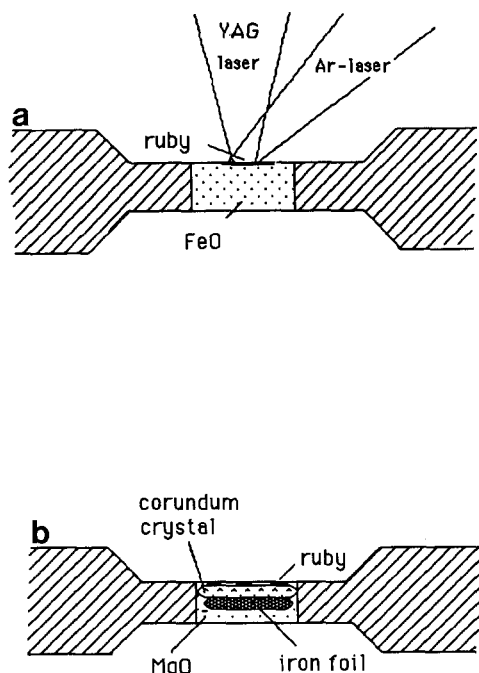
Fig. 1. Sample assembly for experiments of **a** wüstite, **b** iron

that the ruby-fluorescence signal still degrades continually with heating when we put ruby on chemically stable platinum foil. After several times of heating on the platinum, we found a strong ring of ruby-fluorescence at the outer edge of the hot-spot. This ring may be due to the concentration of Cr^{3+} which is consistent with Soret diffusion of Cr under temperature gradient. Therefore degradation of ruby-fluorescence with heating is mainly due to Soret diffusion of Cr rather than the chemical contamination with sample.

Iron. The 99.99% pure iron sample, a foil of 100 μm initial thickness and flattened to about 40 μm thick, was loaded into the gasket hole over a layer of fine-grained MgO powder. A small disc of colorless corundum was put over iron-foil. Several small ruby chips were spread over the assemblage (Fig. 1 b). It is usually necessary to isolate the iron sample from the anvils. In our earlier work (Lazor et al. 1992; Shen et al. 1992), we had used MgO or Al_2O_3 powder as the medium and taken the temperature of melting as soon as the melting was observed. Once the melting begins, a reaction with the powder can be observed. In order to avoid this, we followed the method suggested by Boehler et al. (1990) and used a corundum disc on the top of the sample as the isolator. The use of such a disc retards or eliminates any significant reaction between the sample and the disc. Use of the disc also minimizes the decrease of pressure due to laser heating (fusion of grain boundaries, relaxation of stress etc.).

Pressure Measurements

Wüstite. Modified Mao-Bell type diamond anvil cells were used with type I diamonds. Pressures were measured by ruby-fluorescence technique (Mao et al. 1978). Ruby allows the visual observation of the sample inside the diamond cell and provides a thermal insulation between the sample and the diamond. Pressure can be measured exactly at the spot of the experiment; pressures were measured before and after heating. The magnitude of the pressure decrease following laser heating is about 10–15% of the initial pressure. Usually pressure drops most after first heating; further heating does not change the pressure much (1–3%).

Determination of the pressure on the melting spot during heating requires an accounting of both thermal pressure and relaxation effects. Since the pressure becomes almost stable after first heating, we treat the total pressure as the stabilized pressure plus thermal pressure. A maximum estimate of the pressure increase on laser heating is given by the thermal pressure at constant volume. For temperatures of 2000–3000 K under laser beam, the so-called thermodynamic thermal pressure (Heinz 1990), is estimated to be 50–100 kbar from the P-V-T relations for wüstite. Since the laser beam was quite defocussed, the temperature gradient across the heated spot is much less than 2000 K or 3000 K and because the volume is not constant during heating, the actual thermal pressure should be much less than the estimated value of 50–100 kbar. Heinz (1990) considered the thermal elastic effect on thermal pressure and calculated that the thermal pressure in the thermal elastic case is approximately one-half of the expected thermodynamic thermal pressure. Based on the consideration of the thermal elastic effect (Heinz 1990) and pressure effect on thermal pessure, we assume the magnitude of thermal pressure to be about 7% of the pressure after heating. As is obvious, the measurement of the actual pressure (i.e. in-situ pressure during heating) is not yet possible experimentally with available technique. We consider the thermal pressure estimate as a theoretical task; therefore in this study, we present the raw experimental data on the measured pressure of the quenched sample as well. The pressure uncertainties are approximately ± 10 kbar at 100 kbar and ± 30 kbar at 500 kbar due to pressure gradient across the spot.

Iron. Pressures were measured by fluorescence signals from scattered ruby chips. When MgO or Al_2O_3 powder was used as the pressure medium, the situation is similar to that of wüstite as discussed above. When the corundum disc is used, the magnitude of the pressure decrease following laser-heating is less than that of wüstite. Again we assume the same magnitude of thermal pressure as that of wüstite and treat the pressure after heating plus thermal pressure as representative of the pressure within the sample.

Temperature Measurements

Optical geometry to measure temperatures and pressures in a laser-heated diamond anvil cell has been described in detail by Lazor et al. (1993). The sample is heated by Nd:YAG laser (Coherent, model 76-s) with a maximum power of 33 W. The beam, in the TEM_{00} mode, is attenuated with a polariser and focussed with a lens. The beam is usually defocussed to a degree that melting could be reached with maximum laser power to obtain the lowest possible temperature gradient in the sample. The temperature of laser-heated sample is determined by measuring the thermal radiation emitted by the sample as a function of wavelength in the range from 600 nm to 900 nm and fitted to Planck's radiation function. Wavelength dependence of emissivity was taken into account for fitting. Different wavelength dependence of emissivity in calculation at 3000 K can change the temperature over 200 K.

Since a 50-μm-diameter pinhole at the entrance of the monochrometer is used, we can measure the temperature of the sample area of 3 μm in diameter. The entire set of optics was calibrated with a standard Quartz halogen tungsten lamp (Oriel, model 63361). Temperature fluctuations due to laser power fluctuation were measured for different materials: for nickel, platinum, and FeO at about 1850 K, 2020 K, and 2200 K, respectively. Within 2.5 seconds, the largest fluctuations were ± 35 K for nickel, ± 35 K for platinum, and ± 40 K for FeO; the largest fluctuation was ± 80 K for tungsten at 3200 K. The radial temperature distribution of a hot spot of about 20 μm in diameter was measured. The temperature gradient within the central part was about 20 K/μm. For more details see Lazor et al. (1993).

The melting point of tungsten foil under Ar-gas flow at 1 bar was measured as 3671 K using available tungsten emissivity (De Vos 1954). The melting temperature of platinum at 1 bar was meas-

ured as 2043 K using the available emissivity (Cabannes 1967). Both of them are in agreement with the literature data of 3680 K and 2045 K, respectively.

Characterization of Melting. Melting was detected in situ mainly by watching the fluid-like motion in the molten sample using a beam splitter (10R/90T) and a 488 nm band-pass filter (F2) in front of a CCD camera. With increasing power, we kept watching the texture of the hot-spot by reflected light of Ar-laser and recording the temperature at each step. As the wavelength of Ar-laser (488 nm) is far away from the range of the emission spectra we collect, Ar-laser has no effect on temperature. The visible thermal emission (bright glow) from the hot spot is cut by a movable 488 nm band-pass filter. Therefore the change in texture can be seen in-situ at both high temperatures and high pressures. The first change in texture is considered as indicating melting. This process was repeated at least three times. Usually the size of the spot changing texture had a diameter of 2–5 μm which was just about the corresponding size of the entrance pinhole. A big continuous change in texture was considered to indicate that the melting temperature had exceeded. Note that if we turn off the laser after the first change in texture, we do not observe typical circular feature of melting. This means that the first change in texture cannot be caught without in-situ observation. Therefore in methods where quenching is used, the melting temperature would be overestimated substantially.

Boehler et al. (1990) detected melting of iron by three different methods: recording the power-temperature function, monitoring in-situ the intensity of Ar-laser light reflected from the hot-spot and recording the resistance-temperature function. The reported results with these three methods were consistent. With our recorded data of power and temperature, we also found a small discontinuity in power-temperature function. The temperature at this discontinuity is consistent with the temperature of the first-change in texture. At pressures higher than 400 kbar, the change in texture becomes small. Each careful observation in texture change was compared with the power-temperature function.

Results and Discussion

Wüstite

The experimental results on melting of wüstite at pressures up to 600 kbar are shown in Fig. 2 with the piston-cylinder results of Lindsley (1966), multi-anvil result of Ringwood and Hibberson (1990), laser-heated DAC results of Knittle and Jeanloz (1991) and recent results of Boehler (1992). The melting curve when extrapolated to low pressures matches Lindsley's data. However the melting temperature does not rise as rapidly with pressure as reported by Knittle and Jeanloz (1991). The melting temperature at 600 kbar is about 1200 K lower than theirs. This disagreement can be mainly explained by the different ways of detecting melting as discussed in the previous section. The temperature at the first change in texture can be several hundred degrees lower than that observed after a large change in texture. The recording of the typical melting features require large textual changes which happen only after the melting temperature has exceeded substantially. Therefore it is important that the melting is detected in-situ.

The melting temperature was measured both with increasing and decreasing of pressure. A little discrepancy in melting temperature was found at pressures lower than 200 kbar in these two types of measurements. At higher pressures the results are very close. In Fig. 2,
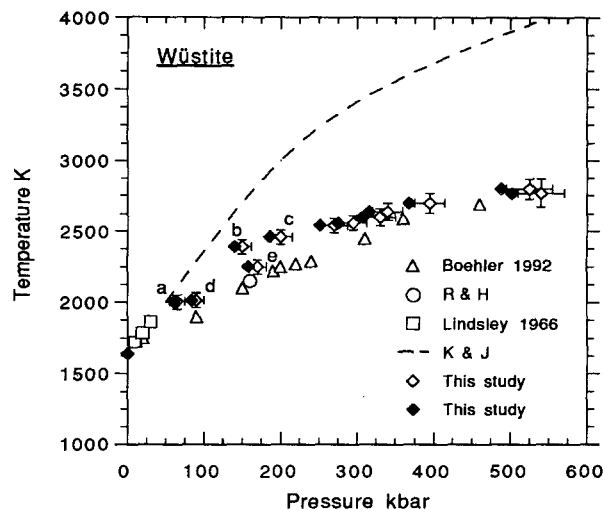

Fig. 2. Experimental results on melting of wüstite with the starting composition $Fe_{0.947}O$. R&H, Ringwood and Hibberson (1990), K&J, Knittle and Jeanloz (1991). The *dashed line* shows melting as measured by Knittle and Jeanloz (1991). The *open diamonds* with error bars (pressure gradient across the heating spot) show the pressures including thermal pressure estimation as discussed in the text. The *solid diamonds* represent the experimental pressure as measured after quenching. *Temperature error bars* show the data scatter at several repeat measurements

points a, b and c were measured with increasing pressure and points d, e with decreasing pressure. If we compare these results with those of Ringwood and Hibberson (1990), the data obtained during decreasing pressure is close to their's. Since at low pressures, chemical reactions between Al_2O_3 and FeO sample is possible, this discrepancy in the two processes could be due to a chemical reaction. At higher pressures, above 200 kbar, oxides become more stable and the consistent results in these two processes imply that chemical reaction at this pressure range on melting can be neglected. The data at pressures above 200 kbar are then more reliable. The present melting data are in good agreement with the work by Boehler (1992) where Ar gas medium was used. The composition of wüstite Fe_xO (x: 0.88–0.95) is a function of pressure and temperature. Many researchers (e.g., McCammon and Liu 1984; Liu 1976; Shen et al. 1983) showed that x increases as a function of pressure below 100 kbar and then decreases with increasing pressure at pressures above 100 kbar. Therefore the experimental result here may represent the melting of wüstite with a composition somewhat different from that of the starting material $Fe_{0.947}O$.

The melting point of wüstite at 1 bar under Ar-gas flow was measured as 1620 ± 20 K; here the error represents the data at several repeating measurements, using the wavelength independent emissivity. The melting temperature at 1 bar was measured to be 1648 K by Darken and Gurry (1946).

Iron

The experimental results on melting of iron in the laser heated DAC at pressures up to 600 kbar are shown in
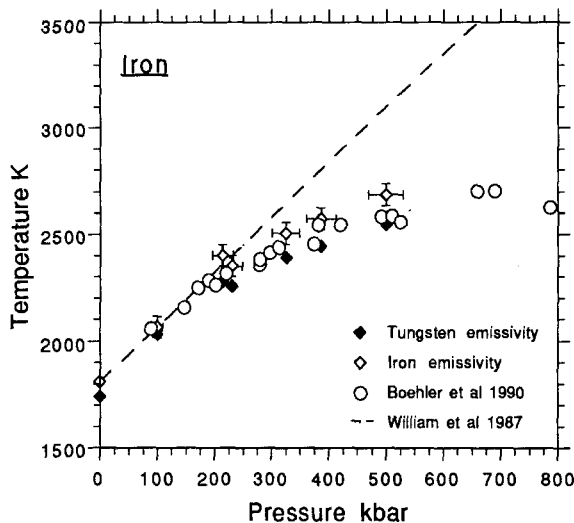
Fig. 3. The experimental results on melting of iron. The *dashed line* represents the melting curve of Williams et al. (1987). *Solid diamonds* denote the results with tungsten emissivity while *open diamonds* represent that with iron emissivity (see discussion in the text). *Solid diamonds* have the same error bars as that of open diamonds. Pressures include thermal pressure estimation. *Pressure error bars* show the pressure gradient across the heating spot; *temperature error bars* represent the data scatter at several repeat measurements

Fig. 3 along with the results of Boehler et al. (1990) and Williams et al. (1987). Both tungsten emissivity and iron emissivity have been used to calculate the melting temperatures. It can be seen that the data with tungsten emissivity (solid diamonds) agree well with that of Boehler et al. (1990), who also used the tungsten emissivity in their calculations. Therefore our data do match their data, which implies that the technique in this study is comparable to their's. However, if tungsten emissivity was used, the measurement of the melting point of iron at 1 bar under Ar-gas flow resulted in a temperature which is about 60 K lower than the literature value of 1808 K. With the iron emissivity data (see discussion below), we recalculated the temperature with the collected data on iron melting at 1 bar and got the temperature value close to 1808 K. The melting temperatures at high pressures were also calculated using the same emissivity data. The results are shown in Fig. 3 with open diamonds with error bars.

Discussions

The determination of temperature by measuring the thermal radiation is dependent on emissivity of the sample. For iron, although some measurements are available on wavelength dependence of the emissivity (Taylor 1952; Cabannes 1967, and references therein), the absolute values of emissivity are scattered. Furthermore, the pressure and temperature effects on wavelength dependence of emissivity are still unknown. Boehler et al. (1990) used tungsten's wavelength dependence of emissivity to calculate the temperature; Williams et al. (1991)

assumed the wavelength dependence of emissivity to be constant. According to our measurement of the melting point of iron at 1 bar, we found it difficult to match the literature data if the tungsten emissivity was used. Here, the linear change in emissivity with wavelength is assumed and given by:

$$\varepsilon = \varepsilon_0 [1 + \varepsilon_1 (\lambda - 750)], \tag{1}$$

where ε is emissivity, ε_0 the emissivity fitting to Planck's function, ε_1 the parameter of the wavelength dependence of emissivity and λ is wavelength in nm. From Taylor (1952) and Cabannes (1967, and references therein), ε_1 was estimated in the range from -5.0×10^{-4} nm^{-1} to -3.0×10^{-4} nm^{-1} from different authors, which is much smaller than the value for tungsten ($\varepsilon_1 = -7.0 \times 10^{-5}$ nm^{-1}). The interval for ε_1 resulted in an error in temperature ranging from ± 10 K at 1900 K to ± 30 K at 2600 K. Since it is difficult to consider the pressure and temperature dependence of emissivity at the present stage of both theory and available data, these emissivity data were used for calculating melting temperatures at high pressures. For wüstite, emissivity data is not available. We corrected the melting temperature of wüstite at 1 bar to 1648 K with $\varepsilon_1 = 7.0 \times 10^{-4}$ nm^{-1}. The melting temperature at high pressures was calculated by using this corrected emissivity. Comparing the temperature with constant emissivity, the temperature is about 60 K higher at 2500 K.

The thermodynamics of wüstite at high pressure and temperature is complicated because the composition may change with pressure and temperature and, as a result, the physical parameters (e.g., thermal expansion coefficient, bulk modulus) can also change (McCammon and Liu 1984). Therefore we need to know the pressure and temperature dependence of the composition to discuss the thermodynamics of wüstite solid solution from the experimental results. Since the available data are with large uncertainties, we assume that the composition of wüstite does not change at different pressures and temperatures. For the starting material, $Fe_{0.947}O$, thermodynamical and thermophysical data are available (Sundman 1991; Coughlin et al. 1951; Yagi et al. 1985; Hazen and Jeanloz 1984; Jackson et al. 1990). With an optimization technique (Saxena and Shen 1992), we have made these data to be internally consistent. The thermodynamic parameters of liquid phase have been optimised by minimizing the total Gibbs free energy. The results are shown in Table 1.

As compared to the previous laser-heated diamond anvil experiments on iron, it is shown in Fig. 3 that at pressure below 200 kbar our results along with that of Boehler et al. (1990) and Williams et al. (1991) are consistent. Above 200 kbar, our results are much closer to those of Boehler et al. (1990). In Fig. 4, the melting curves of wüstite and iron have been plotted using third-order polynomial equations for interpolation, fitted by least squares to data of melting. It can be seen that the melting curve of wüstite shows a higher slope at pressures below 300 kbar and almost the same slope as that of iron at higher pressures. Using the Krant & Kennedy's melting model, McCammon et al. (1983) showed

Table 1. The thermodynamical parameters of wüstite[a]

		Solid	Liquid[h]
$\Delta H(298)$ (J/mol)		-265152[b]	-215158
$\Delta S(298)$ (J/mol·K)		58.7[b]	92.5
V_{298} (cm³/mol)		12.04[c]	13.0
α_p (K⁻¹)	α_0 (10^6)[d]	56.6	59.2
	α_1 (10^8)	0.949	0.005
	α_2 (10^2)	-0.221	-2077
	α_3	-1.53	0
β_T (bar⁻¹)	β_0 (10^6)[e]	0.585	0.952
	β_1 (10^{11})	15.88	-0.886
	β_2 (10^{12})	-0.008	0.155
	β_3 (10^{16})	0.053	-0.353
K'_{OT} (dK/dP)		4.0[f]	3.55
C_p (J/mol·K)	c_0[g]	43.36	47.84
	c_1	0.0117	0
	c_2 (10^{-4})	0.162	0
	c_3 (10^{-6})	-0.671	0
	c_4 (10^{-8})	0.929	0

[a] The results are with the composition of $Fe_{0.947}O$ under the assumption that the composition does not change at different pressures and temperatures

[b] Sundman (1991)

[c] see Fei and Saxena (1986)

[d] Thermal expansion coefficients with equation: $\alpha_p = \alpha_0 + \alpha_1 T^{-1} + \alpha_2 T^{-2} + \alpha_3 T^{-3}$. The data at 300 K from Camichael (1982), at high temperatures the optimization technique of Saxena and Shen (1992) was used

[e] Isothermal compressibility with equation: $\beta_T = \beta_0 + \beta_1 T + \beta_2 T^2 + \beta_3 T^3$; isothermal bulk modulus: $K_T = 1/(\beta_0 + \beta_1 T + \beta_2 T^2 + \beta_3 T^3)$. The data at 300 K from Hazen (1981), at high temperatures the optimization technique of Saxena and Shen (1992) was used

[f] Estimated value for K'_{OT}

[g] The data of heat capacity are from Sundman (1991). Here we refitted the data with equation: $C_p = c_0 + c_1 T + c_2 T^{-1} + c_3 T^{-2} + c_4 T^{-3}$

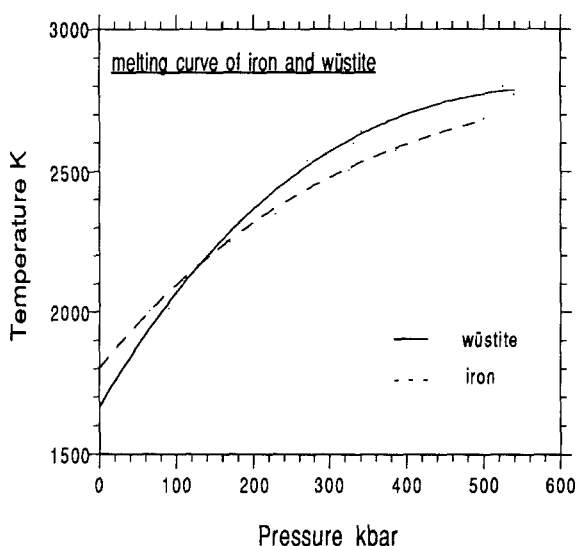[h] Estimated parameters from the results of melting in this study

Fig. 4. Comparison of melting curves of wüstite and iron. The curves were plotted using third-order polynomial equations for interpolation, fitted by least square to data of melting. For iron, the data with iron emissivity was used

that the melting curve of wüstite lies above the melting curve of iron at high pressures. Our results here are in qualitatively agreement with their's. Since oxygen is a possible light element in the outer core (Ringwood 1977), the result of higher melting temperature of wüstite could be geophysically significant. Based on the experiments on the system Fe−FeO at pressures up to 250 kbar, Kato and Ringwood (1989) pointed out that the melting point of iron is decreased considerably by solution of FeO and that the slope of melting curve of Fe−FeO eutectic is much smaller than that of pure iron. With the melting data up to 600 kbar, new constraints can be placed on the phase diagram of the Fe−FeO system.

References

Boehler R, Bargen N von, Chopelas A (1990) Melting, thermal expansion, and phase transitions of iron at high pressures. J Geophys Res 95:21731–21736

Boehler R (1991) EOS 1991 Fall AGU Meeting: p 436

Boehler R (1992) Melting of the Fe−FeO and Fe−FeS systems at high pressures: Constains on core temperatures. Earth Planet Sci Lett 111:217–227

Cabannes F (1967) Facteurs de réflexion et d'emission des metaux. J Phys 28:235–248

Carmichael RS (1982) Handbook of physical properties of rocks. CRC press

Coughlin JP, King EG, Bonnickson KR (1951) High-temperature heat contents of ferrous oxide, magnetite and ferric oxide. J Am Chem Soc 73:3891–3893

Darken LS, Gurry RW (1946) The system iron-oxygen, II, Equilibrium and thermodynamics of liquid oxides and other phases. J Am Chem Soc 68:798

De Vos JC (1954) A new determination of the emissivity of tungsten ribbon. Physica 20:690–714

Fei Y, Saxena SK (1986) A thermochemical data base for phase equilibria in the system Fe−Mg−Si−O at high pressure and temperature. Phys Chem Minerals 13:311–324

Hazen RM (1981) Systematic variation of bulk modulus of wüstite with stoichiometry. Ann Rep Geophys Lab 80:277–280

Hazen RM, Jeanloz R (1984) Wüstite ($Fe_{1-x}O$): A review of its defect structure and physical properties. Rev Geophys 22:37–46

Heinz DL, Jeanloz R (1987) Measurement of the melting curve of $Mg_{0.9}Fe_{0.1}SiO_3$ at lower mantle conditions and its geophysical implications. J Geophys Res 92:11437–11444

Heinz DL (1990) Thermal pressure in the alser-heated diamond anvil cell. Geophys Res Lett 17:1161–1164

Jackson I, Khanna SK, Revcolevschi A, Berthon J (1990) Elasticity, shear-mode softening and high-pressure polymorphism of wüstite($Fe_{1-x}O$). J Geophys Res 95:21671–21685

Kato T, Ringwood AE (1989) Melting relationship in the system Fe−FeO at high pressures: Implications for the composition and formation of the Earth's core. Phys Chem Minerals 16:524–538

Knittle E, Jeanloz R (1991) The high-pressure phase diagram of $Fe_{0.94}O$: a possible constituent of the Earth's core. J Geophys Res 96:16169–16180

Lazor P, Shen G, Saxena SK (1992) EOS 1992 AGU Spring Meeting, p 368

Lazor P, Shen G, Saxena SK (1993) Laser-heated diamond anvil cell experiments at high pressure: Melting curve of nickel up to 700 kbar. Phys Chem Minerals 20:86–90

Lindsley DH (1966) Pressure-temperature relations in the system $FeO-SiO_2$ Yb Carnegie Inst 65:226–230

Liu LG (1976) The high pressure phase of $FeSiO_3$ with implications for Fe_2SiO_4 and FeO. Earth Planet Sci Lett 33:101–106

Mao HK, Bell PM, Shaner JW, Steinberg DJ (1978) Specific volume measurements of Cu, Mo, Pd and Au and calibration of the ruby R1 fluorescence pressure gauge for 0.06 to 1 Mbar. J Appl Phys 49:3276–3283

McCammon CA, Ringwood AE, Jackson I (1983) Thermodynamics of the system $Fe-FeO-MgO$ at high pressure and temperature and a model for formation of the Earth's core. Geophys J R Astr Soc 72:577–595

McCammon CA, Liu LG (1984) The effects of pressure and temperature on nonstoichiometric wüstite, Fe_xO: The iron-rich phase boundary. Phys Chem Minerals 10:106–113

Ringwood AE (1977) Composition of the core and implications for the origin of the Earth. Geochem J 11:111–136

Ringwood AE, Hibberson W (1990) The system $Fe-FeO$ revisited. Phys Chem Minerals 17:313–319

Saxena SK, Shen G (1992) Assessed data on heat capacity, thermal expansion and compressibility for some oxides and silicates. J Geophys Res 97:19813–19825

Saxena SK, Shen G, Lazor P (1993) Thermodynamics of iron and earth's core (in preparation)

Shen P, Bassett WA, Liu LG (1983) Experimental determination of the effects of pressure and temperature on the stoichiometry and phase relations of wüstite. Geochim Cosmochim Acta 47:773–778

Shen G, Lazor P, Saxena SK (1992) EOS 1992 AGU Spring Meeting, p 368

Sundman B (1991) An assessment of the FeO system. J Phase Equilibria 12:127–140

Taylor JE (1952) The variation with wavelength of the spectral emissivity of iron and molybdenum. J Optic Soc Amer 42:33–36

Williams Q, Jeanloz R, Bass J, Svendsen B, Ahrens TJ (1987) The melting curve of iron to 250 giapascals: a constraint on the temperature at the Earth's center. Science 236:181–182

Williams Q, Jeanloz R (1991) The high pressure melting curve of iron: a technical discussion. J Geophys Res 96:2171–2184

Yagi T, Suzuki T, Akimoto S (1985) Static compression of wüstite $(Fe_{0.98}O)$ to 120 GPa. J Geophys Res 90:8784–8788